A pair of light signaling factors FHY3 and FAR1 regulates plant immunity by modulating chlorophyll biosynthesis

Wanqing Wang[1†], Weijiang Tang[1], Tingting Ma[1], De Niu[2], Jing Bo Jin[2], Haiyang Wang[3] and Rongcheng Lin[1,4]*

[1]Key Laboratory of Photobiology, Institute of Botany, the Chinese Academy of Sciences, Beijing 100093, China, [2]Key Laboratory of Plant Molecular Physiology, Institute of Botany, the Chinese Academy of Sciences, Beijing 100093, China, [3]Biotechnology Research Institute, the Chinese Academy of Agricultural Sciences, Beijing 100081, China, [4]National Center for Plant Gene Research, Beijing 100093, China. [†]Current address: College of Biochemical Engineering, Beijing Union University, Beijing 100023, China. *Correspondence: rclin@ibcas.ac.cn

Abstract   Light and chloroplast function is known to affect the plant immune response; however, the underlying mechanism remains elusive. We previously demonstrated that two light signaling factors, FAR-RED ELONGATED HYPOCOTYL 3 (FHY3) and FAR-RED IMPAIRED RESPONSE 1 (FAR1), regulate chlorophyll biosynthesis and seedling growth via controlling *HEMB1* expression in *Arabidopsis thaliana*. In this study, we reveal that FHY3 and FAR1 are involved in modulating plant immunity. We showed that the *fhy3 far1* double null mutant displayed high levels of reactive oxygen species and salicylic acid (SA) and increased resistance to *Pseudomonas syringae* pathogen infection. Microarray analysis revealed that a large proportion of pathogen-related genes, particularly genes encoding nucleotide-binding and leucine-rich repeat domain resistant proteins, are highly induced in *fhy3 far1*. Genetic studies indicated that the defects of *fhy3 far1* can be largely rescued by reducing SA signaling or blocking SA accumulation, and by overexpression of *HEMB1*, which encodes a 5-aminolevulinic acid dehydratase in the chlorophyll biosynthetic pathway. Furthermore, we found that transgenic plants with reduced expression of *HEMB1* exhibit a phenotype similar to *fhy3 far1*. Taken together, this study demonstrates an important role of FHY3 and FAR1 in regulating plant immunity, through integrating chlorophyll biosynthesis and the SA signaling pathway.

INTRODUCTION

Plants have evolved elaborate regulatory mechanisms to cope with adverse abiotic and biotic stresses at the cost of plant growth and development (Bray et al. 2000; Jones and Dangl 2006). In response to biotic stresses, plant cells undergo massive transcriptional reprogramming to activate immune response and resistance pathways. However, constitutive activation of plant immunity impairs growth and fitness. Therefore, in the absence of environmental challenges or when the stress is relieved, the plant immune response must be kept under tight genetic control (Tian et al. 2003).

Recognition of a pathogen effector by a host resistance (R) protein can lead to effector-trigged immunity (ETI), which is characterized by the hypersensitive response (Jones and Dangl 2006). In plants, a suite of R proteins, mainly nucleotide-binding (NB) and leucine-rich repeat (LRR) domain-containing proteins, are the major intracellular receptors that sense pathogen-derived molecules (Caplan et al. 2008; Eitas and Dangl 2010; Heidrick et al. 2012). Activation of NB-LRR R proteins leads to the production of salicylic acid (SA), a plant

defense hormone that plays a central role in defense signaling; the upregulation of expression of *pathogenesis-related* (*PR*) genes; and the induction of systemic acquired resistance (SAR) (Hammond-Kosack and Jones 1996; Shah 2003; Vlot et al. 2009). Thus, overexpression of *R* genes often triggers an autoimmune response (Oldroyd and Staskawicz 1998; Stokes et al. 2002). Two pathways function downstream of the NB-LRR R proteins. ENHANCED DISEASE SUSCEPTIBILITY 1 (EDS1) and its sequence-related interacting partner PHYTOALEXIN DEFICIENT 4 (PAD4) act in basal resistance and ETI initiated by the Toll-like/interleukin 1 receptor (TIR) type NB-LRR R proteins (Vlot et al. 2009). EDS1 and PAD4 also amplify SA signaling via a positive feedback loop (Feys et al. 2001). NONSPECIFIC DISEASE RESISTANCE 1 (NDR1) regulates another subset of R proteins, coiled-coil (CC) type NB-LRR proteins (Century et al. 1997). Upon pathogen challenge, SA biosynthesis is strongly induced via the activity of *SALICYLIC-ACID-INDUCTION DEFICIENT 2* (*SID2*), which encodes chloroplast-localized isochorismate synthase I (ICS1) (Wildermuth et al. 2001). The *Arabidopsis sid2* mutant is defective in pathogen-induced SA synthesis and is severely compromised

in disease resistance (Wildermuth et al. 2001). Increased SA levels induce redox changes and result in the reduction of NON-EXPRESSOR OF PATHOGENESIS-RELATED GENES 1 (NPR1) to a monomeric form that accumulates in the nucleus to activate defense-responsive gene expression, resulting in plant immunity (Fu and Dong 2013).

Increasing evidence suggests that light has a profound influence on plant immunity, and full activation of the defense response to pathogens is often dependent on photoreceptors (Karpinski et al. 2003; Hua 2013). For instance, the *Arabidopsis* phytochrome B (*phyB*) mutant is susceptible to the fungal pathogen *Fusarium oxysporum*, and the *Oryza sativa* (rice) *phyA phyB phyC* triple mutant is susceptible to the blast fungus *Magnaporthe grisea* (Kazan and Manners 2011; Xie et al. 2011). Furthermore, phyA, phyB, and cryptochrome 1 (cry1) photo-receptors are required for SA-regulated gene expression and SAR (Genoud et al. 2002; Wu and Yang 2010). Despite this recent progress, the molecular linkage between light signaling and plant immunity remains poorly understood.

In plants, tetrapyrroles and their derivatives play essential roles in a wide range of biological processes, including photosynthesis, respiration, and signal transduction (Mochizuki et al. 2010; Tanaka et al. 2011). The tetrapyrrole biosynthesis pathway consists of two main branches, i.e., the chlorophyll and heme branches. Previous studies reported that inhibition of several enzymes in the tetrapyrrole biosynthetic pathway induces cell death and/or SAR (Tanaka and Tanaka 2007). For example, transgenic tobacco (*Nicotiana tabacum*) with reduced activity of either uroporphyrinogen decarboxylase (UROD) or coproporphyrinogen oxidase (CPO) and *Arabidopsis* plants expressing an antisense protopor-phyrinogen oxidase gene displayed necrotic leaf lesions, constitutive expression of *PR* genes, high levels of SA accumulation, and increased resistance to pathogens (Mock et al. 1990; Molina et al. 1999). In addition, the maize (*Zea mays*) *les22* mutant with partial deficiency in UROD, the *Arabidopsis* CPO-deficient mutant *lesion initiation 2*, and transgenic tobacco plants with reduced ferrochelatase expression displayed lesion-mimic or necrotic phenotypes (Hu et al. 1998; Ishikawa et al. 2001; Papenbroack et al. 2001). However, the underlying mechanism by which tetrapyrrole biosynthesis contributes to the defense response is largely unknown.

In a previous study, we reported that two homologous transcription factors essential for phyA signaling, FAR-RED ELONGATED HYPOCOTYL 3 (FHY3) and FAR-RED IMPAIRED RESPONSE 1 (FAR1), directly bind to the promoter region of *HEMB1* (which encodes a 5-aminolevulinic acid dehydratase, ALAD) and activate its expression, and thus regulate chlorophyll biosynthesis and seedling growth (Tang et al. 2012). In this study, we found that both the *fhy3 far1* double null mutant and transgenic plants in which *HEMB1* was suppressed by artificial microRNA (amiRNA) display an autoimmune response, including accumulation of SA, strong induction of *PR* genes, and increased resistance to pathogen infection. We showed that overexpression of *HEMB1* largely rescues the *fhy3 far1* phenotype. Our findings suggest that FHY3 and FAR1 negatively regulate SA signaling and plant immunity by regulating *HEMB1* expression, thus providing a possible molecular linkage between light signaling and plant immunity.

RESULTS

The adult *fhy3 far1* double mutants undergo premature cell death

When generating the *fhy3 far1* double mutant in a previous study (Lin et al. 2007), we noticed that its homozygotes grew slowly and had a stunted stature in the adult stage under long-day conditions (16 h light/ 8 h dark), and that this phenotype became even more severe under short-day conditions (8 h light/ 16 h dark) (Figure 1A). However, the *fhy3-4* and *far1-2* single parent mutant plants did not differ much from the No-0 (Nossen) wild type, suggesting that FHY3 and FAR1 play redundant roles in controlling adult plant growth. Most remarkably, *fhy3 far1* leaves developed necrotic lesions, resembling those formed during the hypersensitive response after pathogen entry (Figure 1A).

When stained with trypan blue (which indicates dead cells), the leaves of *fhy3 far1* were stained blue, whereas those of *fhy3* and *far1* plants were barely stained, as were those of the wild type (Figure 1B). 3,3′-diaminobenzidine (DAB) staining showed that high levels of hydrogen peroxide (H_2O_2) were accumulated in the leaves of *fhy3 far1*, but not in those of the *fhy3* or *far1* plants (Figure 1C). These data suggest that loss of both *FHY3* and *FAR1* leads to constitutive activation of cell death and accumulation of reactive oxygen species (ROS).

FHY3 and FAR1 globally repress defense-responsive genes

To determine how FHY3 and FAR1 regulate plant growth and cell death, we conducted a microarray analysis using 28-d-old long-day-grown *fhy3 far1* double mutant and No-0 wild-type plants. Using a *q*-value of <0.05 and a fold change of >2 as a cutoff, a total of 2,891 genes were found to be upregulated and 3,074 genes downregulated in *fhy3 far1* compared with the wild-type plants (Dataset S1). A gene ontology (GO) functional classification of the differentially expressed genes was performed using GOEAST software (Zheng and Wang 2008). GO analysis of biological processes showed that the upregulated genes in *fhy3 far1* are largely involved in the response to biotic and abiotic stresses, and metabolic processes. Notably, genes involved in the plant's responses to chitin, fungi, bacteria, other organisms, and ROS and those regulated by SA-mediated signaling and involved in the defense response were significantly overrepresented in *fhy3 far1* compared with the wild-type genome (Figure 2A). These genes include those encoding transcription factors of the WRKY, MYB, NAC, and ethylene-responsive families, receptor-like kinases, cytochrome P450 family members, and mitogen-activated protein kinase signaling components (Dataset S1). For example, WRKY11, WRKY18, WRKY40, and WRKY60 have been documented as modulating resistance to pathogens (Journot-Catalino et al. 2006; Xu et al. 2006; Pandey et al. 2010). ACCELERATED CELL DEATH 6, a transmembrane protein with cytosolic ankyrin repeats, is involved in regulating both growth and defense traits (Todesco et al. 2010). On the other hand, the downregulated genes are largely involved in regulating cellular, developmental, and biosynthetic proc-esses, consistent with the dwarf phenotype of *fhy3 far1*. We then analyzed how many of the genes involved in the response to pathogen infection were among the differentially regulated genes (Bartsch et al. 2006). We found that 813 out of 1,757 (46.3%) pathogen-induced genes were represented in
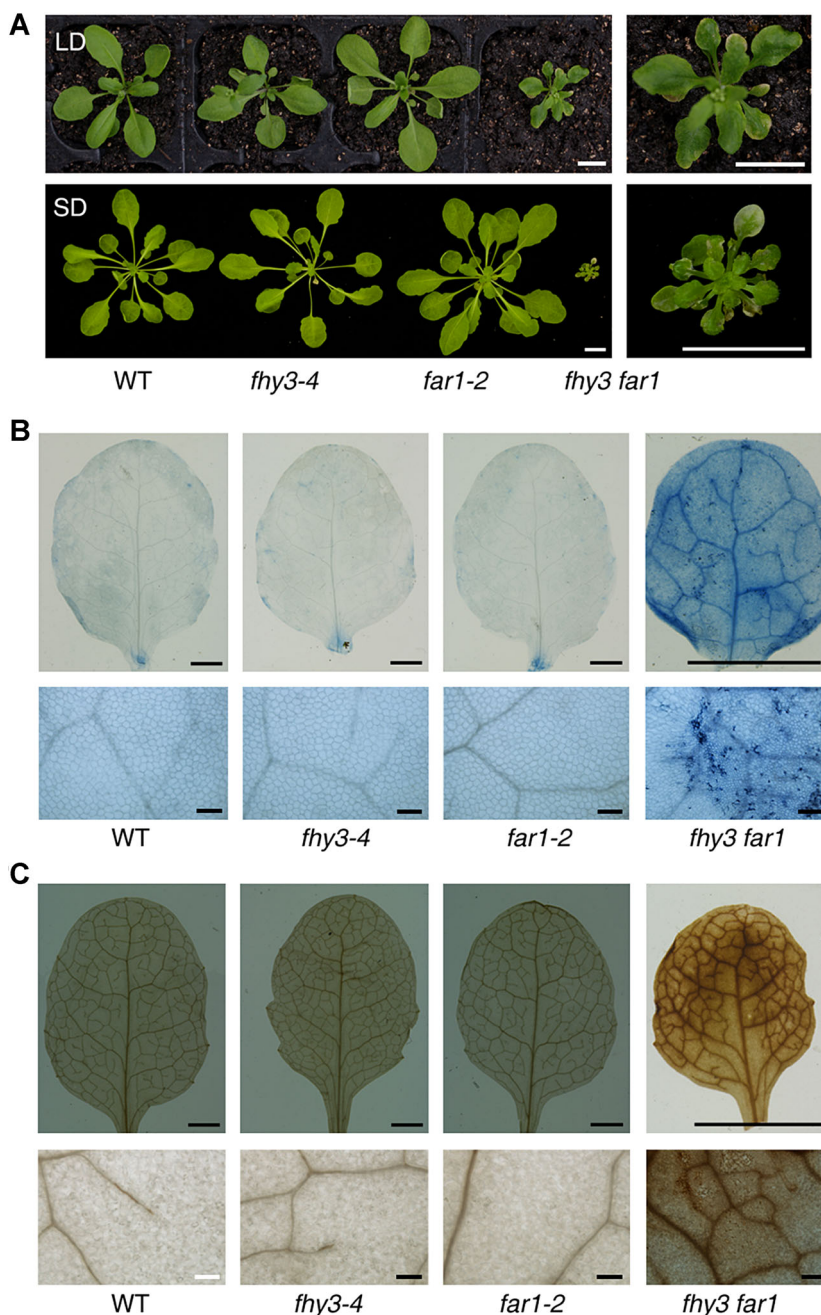
Figure 1. Phenotypic analysis of the *fhy3 far1* double mutant in the adult stage.
(A) Morphology of the No-0 wild type (WT), *fhy3-4*, *far1-2* and *fhy3far1* plants grown on soil under long-day (LD, 16 h light/8 h dark) and short-day (SD, 8 h light/16 h dark) conditions. The photographs were taken when the plants were 4 (LD) and 5 (SD) weeks old. Right panels are magnified photographs of *fhy3 far1*. Bars, 1 cm. **(B)** and **(C)** Trypan blue **(B)** and 3,3'-diaminobenzidine (DAB) **(C)** staining of No-0 WT, *fhy3-4*, *far1-2*, and *fhy3far1* leaves taken from plants grown under LD conditions for 4 weeks. Bars indicate 2 mm in the upper panels and 50 μm in the lower panels.

the upregulated group, while 731 of 2492 (29.3%) pathogen-repressed genes were downregulated in *fhy3 far1* (Figure 2B). Of the 813 genes, 701 (86.2%) are induced by *Pseudomonas syringae* pv *tomato* (*P.s.t.*) DC3000 *AvrRps4* infection in an EDS1-dependent manner (Bartsch et al. 2006). Among the upregulated genes, 145 are believed to respond to SA (total 217 genes) (Blanco et al. 2009).

Interestingly, a total of 64 *R* genes, including 47 TIR-NB-LRR and 17 CC-NB-LRR (Meyers et al. 2003), were found to be induced in *fhy3 far1* (Table 1). Four of these, i.e., PRS6, SNC1, RPP5, and At5G45000, were randomly selected and confirmed to be induced in *fhy3 far* by quantitative reverse transcription-polymerase chain reaction (qRT-PCR). As shown in Figure S1, the expression of these *R* genes was greatly increased in the
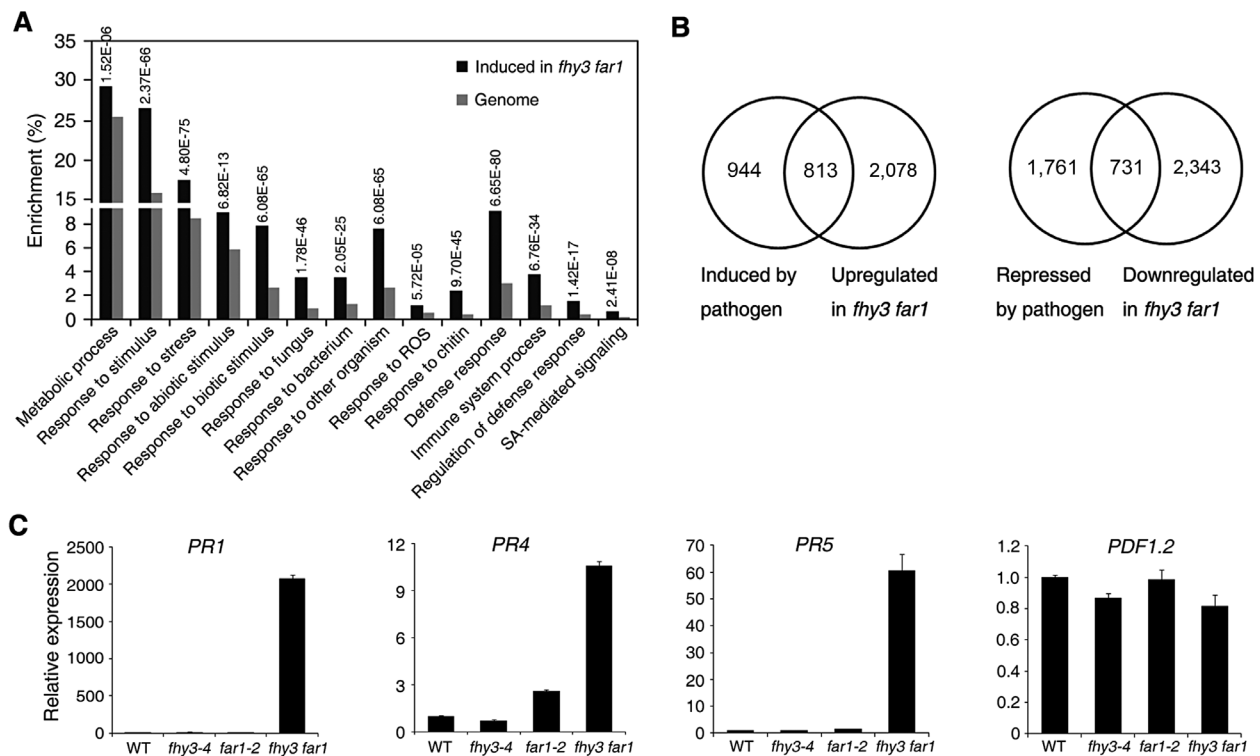
Figure 2. Expression analysis of genes regulated by *FHY3* and *FAR1*
(A) Enrichment of selected categories of gene ontology (GO) biological processes in genes up-regulated in *fhy3 far1* compared to the wild-type genome. The *P*-value of enrichment is calculated as the hypergeometric probability of obtaining so many probes/probesets/genes for a GO term, under the null hypothesis that the probes/probesets/genes were randomly selected from the microarray/genome. **(B)** Venn diagrams showing the overlap of differentially regulated genes in *fhy3 far1* with previously reported pathogen-regulated genes (Bartsch et al. 2006). **(C)** Expression of *PRs* and *PDF1.2* in the No-0 wild type (WT), *fhy3-4*, *far1-2*, and *fhy3 far1* as determined by quantitative RT PCR (qRT-PCR). Plants were grown for 4 weeks under LD conditions. Relative expression was normalized to the level of *UBQ1*. Bars indicate the standard deviation (*SD*) of three biological replicates.

fhy3 far1 double mutant compared with the wild type, but increased to a lesser extent in the parent single mutants. Similarly, the transcript levels of *PR* genes, including *PR1*, *PR4*, and *PR5*, were greatly upregulated in *fhy3 far1*, but not in the *fhy3* and *far1* single mutants (Figure 2C). However, the level of *PDF1.2*, a molecular marker of the jasmonic acid-mediated defense pathway, was not affected by these mutations (Figure 2C). Together, these results indicate that FHY3 and FAR1 are involved in the defense response, likely through regulating the NB-LRR-mediated SA signaling pathway.

FHY3 and FAR1 negatively regulate SA accumulation and disease resistance
We next examined how the SA synthesis and signaling pathway were affected by FHY3 and FAR1. Our qRT-PCR analysis of genes involved in the SA pathway showed that the expression levels of *EDS1*, *PAD4*, *SID2*, and *EDS5* were increased by more than fivefold in the *fhy3 far1* mutant, while the transcripts of *NPR1* and *NDR1* were moderately upregulated. The expression of these genes was also slightly increased in the *far1* single mutant (Figure 3A).

We then evaluated whether SA synthesis was altered in these mutant plants. Total SA and free SA were analyzed by high-performance liquid chromatography. As shown in

Figure 3B and C, the *fhy3 far1* plants accumulated significantly higher levels of free SA (~10 fold) and total SA (free SA plus glucose-conjugated SA, ~20 fold) than the *fhy3* and *far1* single mutant and the wild-type plants, suggesting that FHY3 and FAR1 together repress SA production.

Since SA is one of the most important signaling molecules in plant defense, we tested the mutant and wild-type leaves for resistance to a model pathogen, *P.s.t.* DC3000. Three days after infiltration or spraying, bacterial growth of *P.s.t.* DC3000 on *fhy3 far1* plants was much less than on wild-type or *fhy3* and *far1* plants (Figures S2, 4). Furthermore, growth of *P.s.t.* DC3000 expressing the effector *AvrRps4* (recognized by the TIR-NB-LRR R protein RPS4), and to a lesser extent of *P.s.t.* DC3000 expressing *AvrRpt2* (recognized by the CC-NB-LRR R protein resistant to *P.s.* protein2) was significantly inhibited in the *fhy3 far1* leaves (Figure 4). These results suggest that the defense responses are constitutively activated in *fhy3 far1* and that FHY3 and FAR1 regulate basal defense and resistance.

Mutations in *PAD4*, *EDS1* and *SID2* largely alleviate the *fhy3 far1* defects
To test whether the constitutive defense response in *fhy3 far1* is dependent on the SA biosynthesis or signaling

Table 1. List of *R* genes upregulated in the *fhy3 far1* mutant

Probe code	Gene name	Fold change	*P*-value
TIR-NB-LRR genes			
A_84_P185874	RMG1	47.823	9.48E-05
A_84_P19706	AT5G45000	32.31325	0.027859
A_84_P229729	AT2G20142	24.19823	2.58E-04
A_84_P11332	AT1G17615	18.351322	6.55E-03
A_84_P13393	AT1G66090	16.29933	9.07E-04
A_84_P15928	AT5G46520	12.0586	0.001391
A_84_P11078	AT4G16920	11.30811	1.89E-04
A_84_P849144	AT5G41750	9.761409	3.72E-05
A_84_P10768	AT3G04220	8.293957	1.65E-04
A_84_P19688	AT5G40060	6.82695	2.23E-03
A_84_P14031	AT5G44920	6.689585	5.57E-04
A_84_P18998	AT1G72900	6.625833	4.78E-04
A_84_P20045	AT1G57630	6.105525	0.043992
A_84_P13792	AT4G09430	6.090731	0.007396
A_84_P844198	RPP5	5.780693	1.89E-04
A_84_P157715	TIR	5.220458	0.023633
A_84_P850884	RPP1	4.930057	1.27E-04
A_84_P257040	RPP4	4.846021	4.87E-04
A_84_P799368	AT3G44400	4.798215	2.29E-04
A_84_P20437	AT4G19530	4.333743	0.001867
A_84_P18191	AT2G16870	3.607882	0.0053
A_84_P13978	AT5G22690	3.481065	4.59E-05
A_84_P22532	AT5G41740	3.411526	6.07E-04
A_84_P754645	AT1G31540	3.34389	0.003635
A_84_P12023	AT4G16930	3.212421	4.56E-04
A_84_P10132	AT4G16900	3.197131	0.013832
A_84_P859782	AT1G72890	3.183353	0.002871
A_84_P11714	AT3G04210	3.175821	0.013123
A_84_P851315	AT1G63750	3.15323	0.005253
A_84_P23431	AT5G18370	3.043914	0.001417
A_84_P23371	SNC1	2.972829	5.55E-04
A_84_P833327	AT1G69550	2.911294	0.005158
A_84_P844467	AT3G44670	2.895682	1.66E-04
A_84_P831991	AT2G14080	2.809864	0.001404
A_84_P22782	AT1G72950	2.77039	0.002835
A_84_P840641	AT1G17600	2.701304	0.011694
A_84_P13092	AT5G46450	2.482496	1.24E-04
A_84_P825937	AT4G16960	2.4293	0.001445
A_84_P14037	RPS6	2.413073	0.010444
A_84_P11793	AT3G44630	2.401762	1.28E-05
A_84_P18910	AT1G27180	2.372493	9.91E-04
A_84_P22659	AT1G56540	2.27858	7.37E-04
A_84_P819483	AT1G72920	2.276629	0.003455
A_84_P17819	AT5G46270	2.1798034	3.10E-05
A_84_P18775	AT5G48780	2.140335	0.002571
A_84_P16726	AT4G36140	2.067147	3.89E-04
A_84_P134545	CHS1	2.0247023	1.64E-02
CC-NB-LRR genes			
A_84_P15324	ADR1	26.407757	2.42E-04
A_84_P762972	AT4G14610	12.564014	8.57E-04
A_84_P750611	AT1G50180	8.214066	2.80E-04
A_84_P233429	AT1G58390	7.246682	2.86E-05
A_84_P19551	ADR1-L1	6.4361086	2.04E-03
A_84_P22827	RFL1	5.951576	2.11E-03
A_84_P839521	CW9	5.437317	1.76E-03

(Continued)

Table 1. (Continued)

Probe code	Gene name	Fold change	*P*-value
A_84_P22445	ADR1-L2	3.9967146	2.65E-03
A_84_P17213	AT1G58410	3.792377	3.48E-02
A_84_P17424	AT3G14470	3.2127194	8.76E-05
A_84_P23167	ZAR1	2.755153	1.30E-02
A_84_P15917	AT5G43730	2.742159	0.030905
A_84_P21612	AT5G48620	2.4769285	0.0072576
A_84_P19791	AT5G66910	2.432915	0.012265
A_84_P832596	AT5G66900	2.207749	0.002275
A_84_P18728	AT5G35450	2.1631396	6.41E-04
A_84_P173341	AT1G12290	2.113111	0.001391

pathway, we introduced either the *pad4*, *eds1*, or *sid2* mutation into *fhy3 far1* by genetic crossing. Homozygous plants were used in the following studies. The addition of the *pad4*, *eds1* or *sid2* mutation largely suppressed the dwarfism phenotype of *fhy3 far1* (Figure 5A). Furthermore, the transcript levels of *PR1* of the *pad4 fhy3 far1*, *eds1 fhy3 far1*, and *sid2 fhy3 far1* triple mutants were almost completely restored to the level of the wild-type plants (Figure 5B). Moreover, we observed that the sensitivities of these triple mutants to *P.s.t.* DC3000 or *P.s.t.* DC3000 *AvrRps4* infection were similar to those of the *pad4*, *eds1* or *sid2* single mutants (Figure 5C). The SA levels in *pad4 fhy3 far1* and *sid2 fhy3 far1* were also restored to the levels of wild-type plants (Figure 5D). These results indicate that the constitutive defense response of *fhy3 far1* requires functional PAD4, EDS1 or SID2, and thus PAD4, EDS1 and SID2 act downstream of FHY3 and FAR1.

In addition, we introduced the *nahG* transgene, which encodes the bacterial salicylate hydroxylase that blocks SA accumulation and SAR (Gaffney et al. 1993), into *fhy3 far1*. The small-size morphology of *fhy3 far1* was partially suppressed by *nahG* in the *nahG fhy3 far1* plants (Figure 5A), further supporting an essential role of over accumulated SA in triggering the constitutive defense response in *fhy3 far1* double mutants.

Overexpression of *HEMB1* largely rescues the *fhy3 far1* phenotype

We previously generated plants overexpressing *HEMB1* in the *fhy3 far1* mutant background, and found that the leaves of most lines became pale and died at the adult stage (Tang et al. 2012). We screened a large population of the transgenic plants and obtained four independent lines (line *OE-2* and *OE-33* are shown in this study). The heterozygous transgenic plants had 9–17 fold increases in *HEMB1* levels compared to the wild type. Remarkably, the dwarfism phenotype of *fhy3 far1* was largely suppressed in these heterozygous transgenic lines (Figures 6A, S3A). Surprisingly, one-fourth progenies of these heterozygotes had pale leaves and died later. These plants had low levels of *HEMB1* mRNA, due to co-suppression by exogenous *HEMB1* (Figure S3A). In the heterozygous plants, the ALAD activity was recovered to beyond wild-type levels (Figure S3B). Moreover, overexpression of *HEMB1* also largely complemented the aberrant phenotype of *fhy3 far1*, including the cell death response,
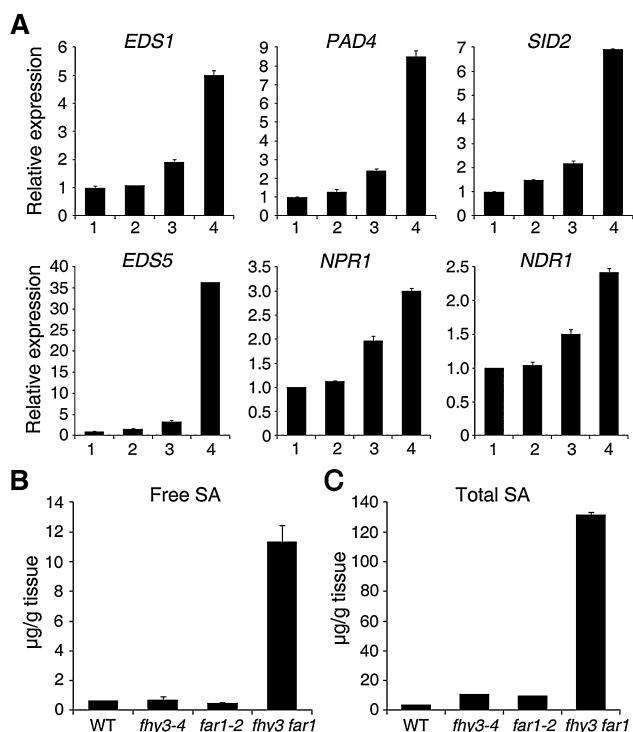
Figure 3. FHY3 and FAR1 together negatively regulate salicylic acid (SA) signaling and its biosynthesis
(A) Expression analysis of genes involved in the SA biosynthesis and signaling pathway in the No-0 wild type (WT), *fhy3-4, far1-2* and *fhy3 far1* mutants. Plants were grown for 4 weeks under long day (LD) conditions. Lane 1, No-0 wild type; lane 2, *fhy3-4*; lane 3, *far1-2*; and lane 4, *fhy3 far1*. Relative expression was normalized to the level of *UBQ1*. Bars indicate the standard deviation (*SD*) of three biological replicates. **(B)** and **(C)** Free SA **(B)** and total SA **(C)** levels in the indicated genotypes grown under LD conditions for 4 weeks, as determined by high-performance liquid chromatography. Bars indicate the *SD* of three replicates.

ROS accumulation, increased expression of *EDS1, PAD4, SID2,* and *PR5*, increased SA production, and increased pathogen resistance to *P.s.t.* DC3000 and *P.s.t.* DC3000 *AvrRps4* (Figure 6B–F). These data together confirm that FHY3 and FAR1 control the autoimmune response largely in a *HEMB1*-dependent manner, consistent with the direct target of these factors.

Reduction of *HEMB1* leads to constitutive activation of the immune response

The above results led us to examine whether *HEMB1* itself is involved in the defense response. To this end, we screened more than 200 independent transgenic lines expressing an artificial microRNA of *HEMB1* (*amiRNA-HEMB1*) in the No-0 wild-type background. It should be noted that most of the homozygous seedlings were seedling lethal due to severe inhibition of *HEMB1* expression and tetrapyrrole biosynthesis, as previously reported (Tang et al. 2012). We obtained three independent lines that developed true leaves and set seeds. The endogenous *HEMB1* levels of *amiRNA-HEMB1* (lines *amiR-1* and *amiR-2* are shown) were reduced to 40%–50% of those in the wild type (Figure S4A). Furthermore, the ALAD activity was drastically impaired in these transgenic lines (Figure S4B).

Similar to the *fhy3 far1* mutant, these *amiRNA-HEMB1* plants were small with a lesion-mimic phenotype (Figure 7A). Trypan blue and DAB staining analyses showed that the *amiRNA-HEMB1* leaves exhibited severe cell death and accumulated high amounts of ROS, respectively (Figure 7B, C). The expression of *EDS1, PAD4, SID2,* and *PR1*, but not of *NDR1*, was dramatically upregulated in both transgenic lines compared with the wild-type control (Figure 7D). Furthermore, these transgenic plants accumulated free SA levels that were approximately 8–11-fold higher than those in the wild type (Figure 7E). When the plants were infiltrated with *P.s.t.* DC3000, bacterial growth on *amiR-1* and *amiR-2* was much less than on the No-0 wild type (Figure 7F). Taken together, these data indicate that a reduction of *HEMB1* leads to a constitutive immune response as do the *FHY3* and *FAR1* mutations.
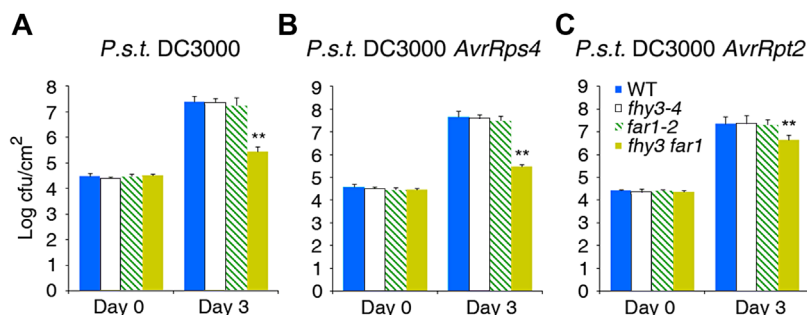

Figure 4. Loss of *FHY3* and *FAR1* causes increased resistance to *Pseudomonas* syringae bacteria
(A–C) Growth of *P.s.t.* DC3000 **(A)**, *P.s.t.* DC3000 *AvrRps4* **(B)**, and *P.s.t.* DC3000 *AvrRpt2* **(C)** on wild type (WT), *fhy3-4, far1-2* and *fhy3 far1* leaves. Leaves of 4-week-old long day (LD)-grown plants were infiltrated with bacterial suspensions at a density of 1×10^5 cfu/mL. Bacterial titers were measured on day 0 and day 3. Bars indicate the standard deviation (*SD*) of four parallel samples. Asterisks denote statistically significant differences in bacterial growth compared with WT (*P* < 0.01, Student's *t*-test). Similar results were obtained in two independent experiments.
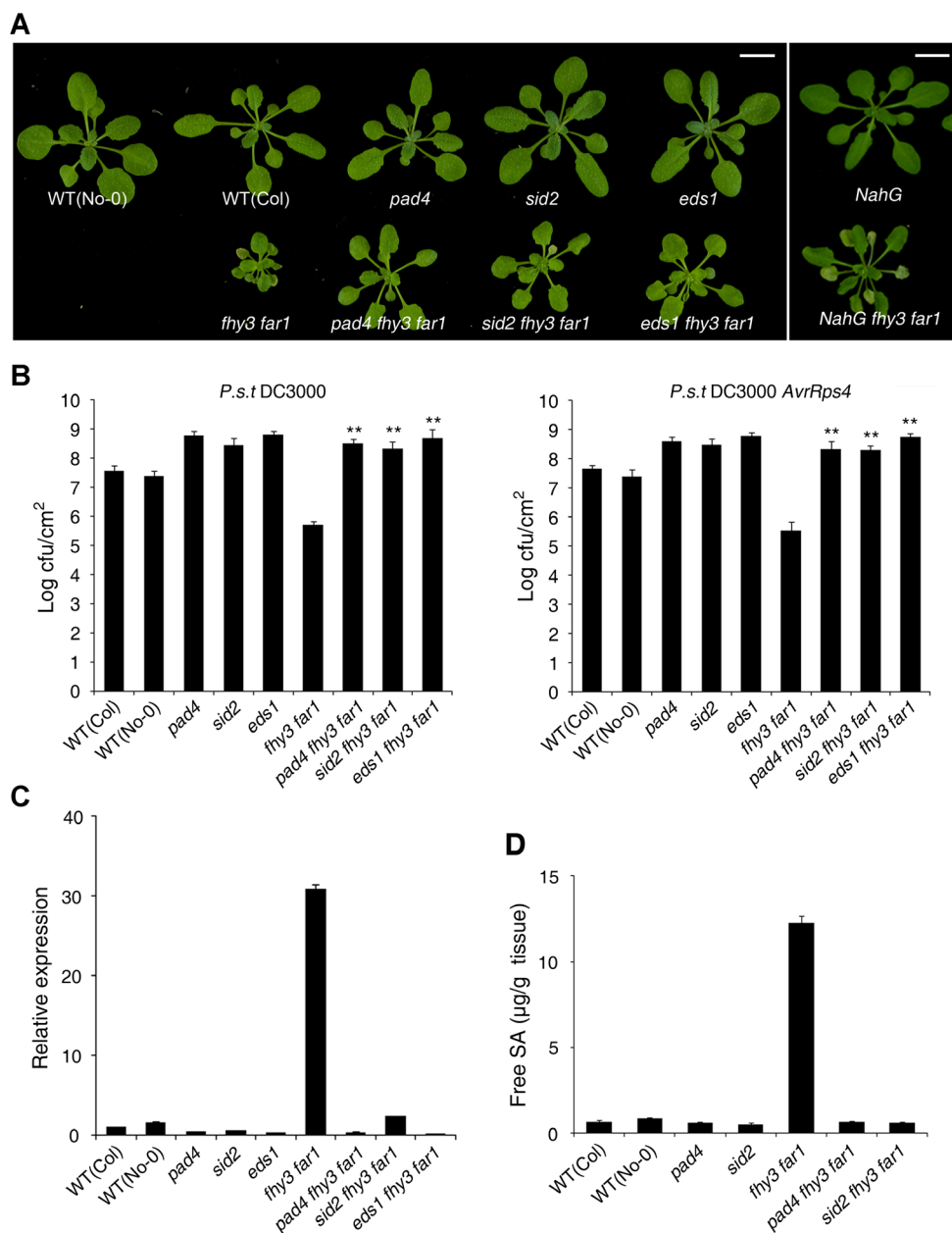
Figure 5. Suppression of the *fhy3 far1* mutant phenotype by *pad4*, *eds1*, and *sid2* mutations
(A) Morphological phenotypes of the wild-type and various mutant plants. Bars: 1 cm. **(B)** Growth of bacteria after infection. Leaves were infiltrated with bacterial suspensions at a density of 1×10^5 cfu/mL for *P.s.t.* DC3000 and *P.s.t.* DC3000 *AvrRps4*. Bacterial titers were measured on day 3. Bars indicate the standard deviation (*SD*) of four parallel samples. Asterisks denote statistically significant differences in bacterial growth compared with *fhy3 far1* double mutant ($P < 0.01$, Student's *t*-test). Similar results were obtained in three independent experiments. **(C)** *PR5* expression. Relative *PR5* expression was normalized to the level of *UBQ1*. Bars indicate SD of three biological replicates. **(D)** Free salicylic acid (SA) levels. Bars indicate the *SD* of three replicates. For A to D, plants were grown under long day (LD) conditions for 4 weeks.

DISCUSSION

FHY3 and FAR1 negatively modulate plant immunity by regulating *HEMB1* expression and SA signaling

In this study, we showed that loss of both *FHY3* and *FAR1* resulted in autoimmune responses, including a dwarfism phenotype with premature cell death, accumulation of ROS

and SA, and resistance to *P. syringae* infection. These responses of *fhy3 far1* are similar to those observed for gain-of-function mutants of *R* genes, such as *snc1* and *ssi4* (Shirano et al. 2002; Zhang et al. 2003). Microarray analysis revealed that FHY3 and FAR1 negatively regulate large numbers of stress- and defense-responsive genes, especially those involved in the SA signaling pathway, e.g., *EDS1*, *SID2*, *PAD4*, and *NDR1*. Consistently, a large
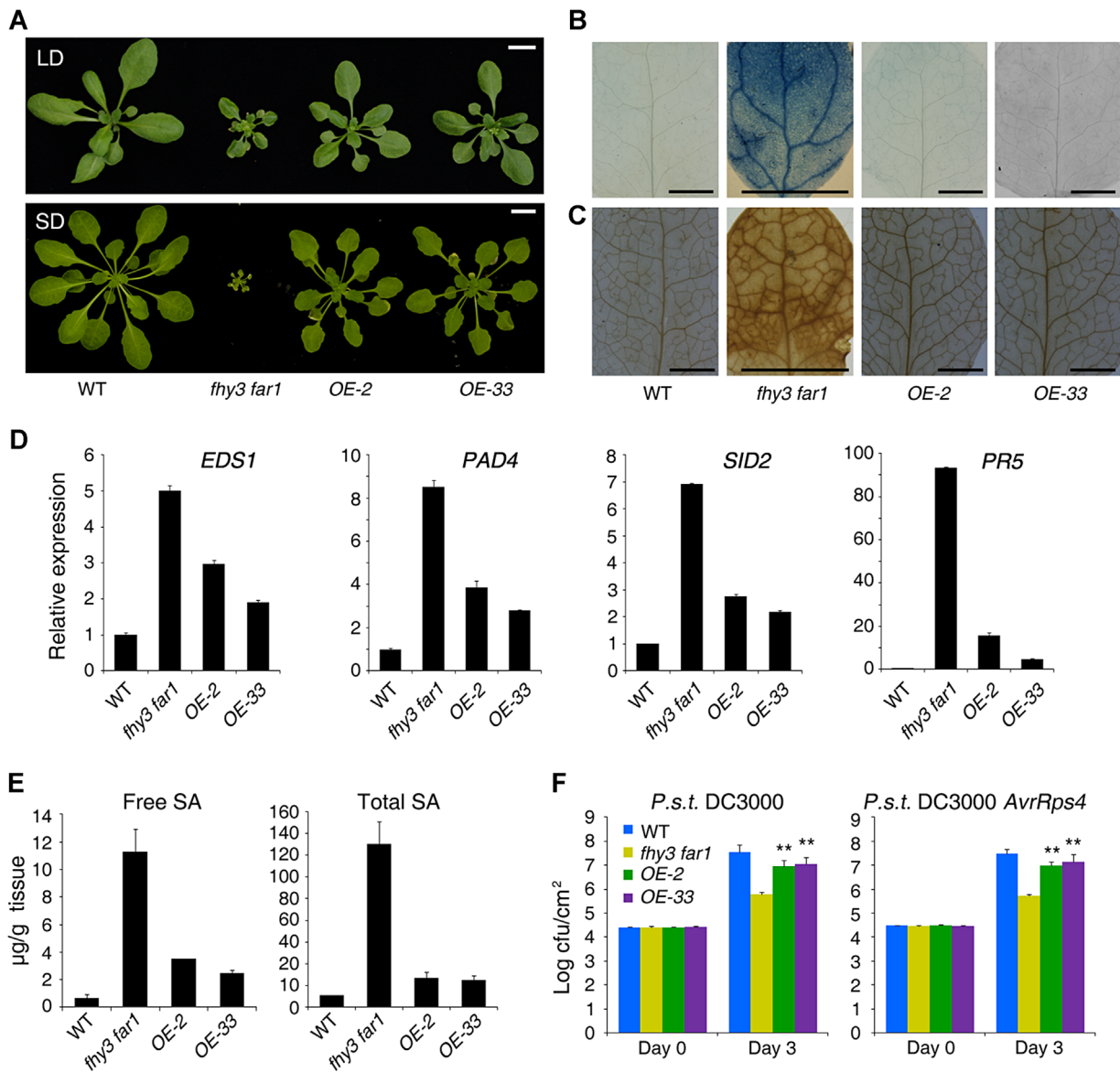
Figure 6. Constitutive expression of *HEMB1* largely rescues the *fhy3 far1* phenotype
(A) Morphology of the wild type (WT), *fhy3 far1*, and two transgenic lines overexpressing *HEMB1* in the *fhy3 far1* mutant background (lines *OE-2* and *OE-33* are shown). Plants were grown in soil under long day (LD) conditions for 4 weeks and under short day (SD) conditions for 5 weeks. Bars, 1 cm. **(B)** and **(C)** Trypan blue **(B)** and 3,3'-diaminobenzidine (DAB) **(C)** staining of leaves of the indicated genotypes. Plants were grown under LD conditions for 4 weeks. Bars, 2 mm. **(D)** Gene expression, as determined by quantitative reverse transcription polymerase chain reaction (qRT-PCR). Relative expression was normalized to the level of *UBQ1*. Bars indicate the standard deviation (SD) of three biological replicates. **(E)** Free and total SA levels in the indicated genotypes. Bars indicate the SD of three replicates. **(F)** Growth of *P.s.t.* DC3000 and *P.s.t.* DC3000 *AvrRps4* on the indicated genotypes. Leaves of 4-week-old plants were infiltrated with bacterial suspensions at a density of 1×10^5 cfu/mL. Bacterial titers were measured on day 0 and day 3. Bars indicate the SD of four parallel samples. Asterisks denote statistically significant differences in bacterial growth compared with *fhy3 far1* double mutant ($P < 0.01$, Student's *t*-test). Similar results were obtained in three independent experiments.

portion of the TIR-NB-LRR and CC-NB-LRR type *R* genes were induced by *FHY3* and *FAR1* mutations. Most intriguingly, growth of *P.s.t.* DC3000, *P.s.t.* DC3000 *AvrRps4* and *P.s.t.* DC3000 *AvrRpt2* was significantly inhibited in the *fhy3 far1* leaves. Furthermore, our genetic data indicate that PAD4, EDS1 and SID2 act downstream of FHY3 and FAR1. Our collective evidence

supports the conclusion that FHY3 and FAR1 are negative regulators of plant immunity.

We previously demonstrated that *HEMB1* is a direct target of FHY3 and FAR1 (Tang et al. 2012). This study further reveals that FHY3 and FAR1 function in the plant immune response, most likely through activating *HEMB1* expression, as the autoimmune
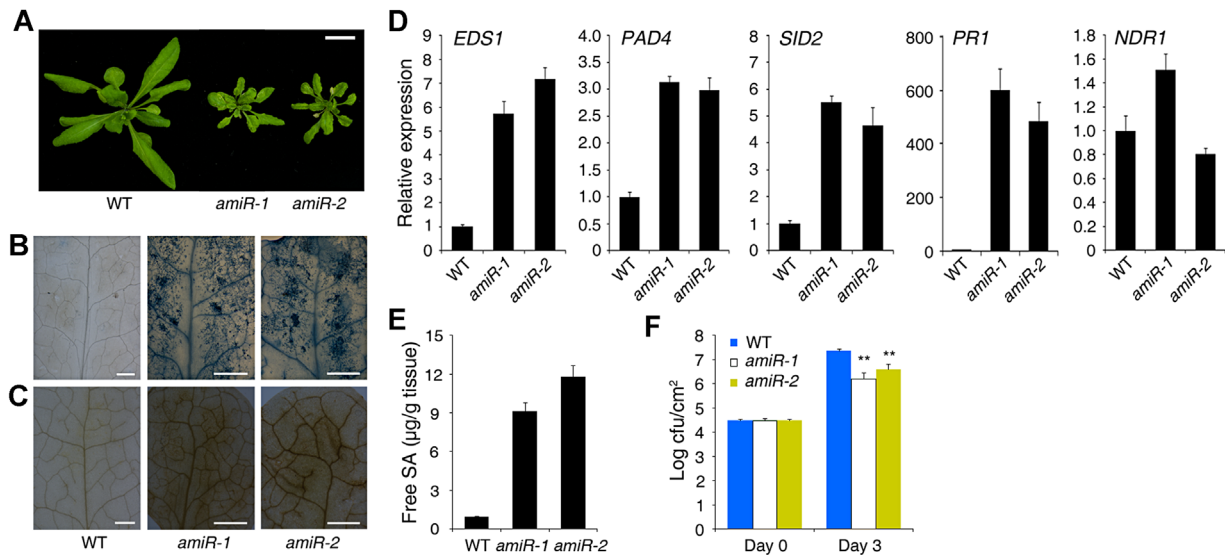
Figure 7. Reduction of *HEMB1* mimics the *fhy3 far1* mutant phenotypes
(A) Morphological phenotype of the No-0 wild type (WT) and two transgenic lines expressing an artificial microRNA of *HEMB1* (lines *amiR-1* and *amiR-2*). Bar, 1 cm. **(B)** and **(C)** Trypan blue **(B)** and 3,3-diaminobenzidine (DAB) **(C)** staining of leaves in the indicated genotypes. Bars, 2 mm. **(D)** Gene expression analysis by quantitative reverse transcription polymerase chain reaction (qRT-PCR). Relative expression was normalized to the level of *UBQ1*. Bars indicate the standard deviation (*SD*) of three biological replicates. **(E)** Free SA level in the indicated genotypes. Bars indicate the *SD* of three replicates. **(F)** Growth of on the leaves of wild-type and *amiRNA-HEMB1* plants. Leaves were infiltrated with suspensions of *P.s.t.* DC3000 at a density of 1×10^5 cfu/mL. Bacterial titers were measured on day 0 and day 3. Bars indicate the *SD* of three parallel samples. Asterisks denote statistically significant differences in bacterial growth compared with WT ($P < 0.01$, Student's *t*-test). Similar results were obtained in two independent experiments. All plants were grown in soil under LD conditions for 4 weeks before examination.

phenotypes of *fhy3 far1* are largely complemented by over-expression of *HEMB1* (Figure 8). In agreement with this proposition, the *amiRNA-HEMB1* transgenic plants exhibited similar autoimmune phenotypes as *fhy3 far1*. Other undefined targets or pathways downstream of FHY3/FAR1 could also be involved in the plant immune response (Strawn et al. 2007).

Although some photoreceptors have been shown to affect defense response (Genoud et al. 2002; Wu and Yang 2010; Kazan and Manners 2011; Xie et al. 2011), the intermediate linkage between them is still missing. FHY3 and FAR1 were derived from an ancient transposase and function as key positive regulators downstream of the phytochrome A signaling pathway, where FHY3 and FAR1 directly binding to the promoters of *FHY1* and *FHL*, whose produces interact with phyA and facilitate its nucleus-cytosol translocation (Hudson et al. 1999; Wang and Deng 2002; Hiltbrunner et al. 2005; Lin et al. 2007). Together with this study, we propose that FHY3 and FAR1 might act as a cross-talk point that integrates light and SA signaling. Besides the function in photomorphogenesis and plant immunity, FHY3 and FAR1 play roles in regulating flowering time and the circadian clock (Allen et al. 2006; Li et al. 2011), chloroplast development (Ouyang et al. 2011), chlorophyll biosynthesis (Tang et al. 2012), shoot branching (Stirnberg et al. 2012), and abscisic acid-mediated responses (Tang et al. 2013). In agreement with this, the expression of FHY3 and/or FAR1 themselves is regulated by multiple environmental and endogenous cues. Hence, FHY3 and FAR1 appear to constitute key transcriptional signaling factors that coordinate the expression of downstream genes to ensure
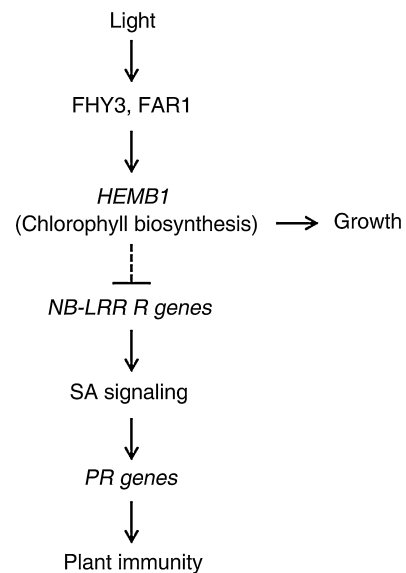

Figure 8. A model showing the role of FHY3 and FAR1 in regulating plant immunity
FHY3 and FAR1 directly promote *HEMB1* expression, leading to the repression of *R* gene expression and SA signaling, and inhibition of plant immunity. On the other hand, *HEMB1* is required for chlorophyll biosynthesis and plant growth. Therefore, FHY3 and FAR1 modulate the balance between plant growth and immunity. Arrows show activation and bar-ended lines denote inhibition.

optimal plant growth, development, and immunity, in response to diverse internal and external signals.

Involvement of tetrapyrrole biosynthesis in plant immunity
Chloroplasts have a critical role in the transcriptional regulation of plant immune signaling (Nomura et al. 2012). This study reveals that *HEMB1*, encoding enzymes in tetrapyrrole (e.g., chlorophyll) biosynthesis, is involved in plant immunity, thus substantiates the link between this biosynthesis pathway and SA-dependent defense responses. There are several possible explanations for the involvement of tetrapyrrole biosynthesis in the defense response. First, those photosensitizing intermediates of the tetrapyrrole pathway could generate ROS upon light irradiation, subsequently leading to plant cell death and defense responses (Reinbothe et al. 1996; Tanaka and Tanaka 2007). For instance, *FLU* encodes a negative regulator of chlorophyll biosynthesis. The conditional *flu* mutant releases singlet oxygen in the chloroplasts and triggers accumulation of free SA and activation of PR genes (Ochsenbein et al. 2006). In this study, the altered biosynthesis of tetrapyrrole compounds in the *fhy3 far1* and *amiRNA-HEMB1* plants leads to ROS production in chloroplasts and this might trigger activation of the SA pathway and plant immunity.

Second, intermediates of tetrapyrrole metabolism, such as ALA, Mg-protoporphyrins, and heme, are considered as potential chloroplast-derived retrograde signaling molecules that modulate photosynthetic gene expression in the nucleus (Strand et al. 2003; Woodson et al. 2011; Czarnecki et al. 2012). In the *fhy3 far1* mutants and *amiRNA-HEMB1* plants, the constitutive over-accumulation of ALA could activate a retrograde signal to regulate nuclear gene expression. Similarly, in isoprenoid biosynthesis, the plastidial metabolite methylerythritol cyclodiphosphate acts as a signal that elicits the expression of stress-responsive genes and elevates SA biosynthesis in response to abiotic stresses (Xiao et al. 2012). Third, SA is synthesized in chloroplasts via the chorismate pathway in *Arabidopsis* (Strawn et al. 2007; Wiermer et al. 2007). Impairment of tetrapyrrole synthesis and chloroplast function and integrity possibly affect SA metabolism. For instance, mutations in genes encoding chloroplast-localized proteins alter SA synthesis and defense signaling (Kachroo et al. 2001; Nomura et al. 2012). Nevertheless, the underlying mechanism by which tetrapyrrole biosynthesis contributes to the plant immune response requires further investigation.

Tetrapyrrole biosynthesis is crucial for plant growth and development, e.g., chlorophylls for photosynthesis, its intermediates also play important roles in regulating plant immunity. Meanwhile, the chloroplasts are sensitive to biotic and abiotic stresses. Therefore, under changing environmental conditions, the tetrapyrrole biosynthetic pathway could fine-tune the antagonistic relationship between growth and immunity in plants.

MATERIALS AND METHODS

Plant materials and growth conditions
The *fhy3-4*, *far1-2*, and *fhy3 far1* mutants are of the *Arabidopsis thaliana* Nossen (No-0) ecotype (Hudson et al. 1999; Wang and Deng 2002; Lin et al. 2007). The *eds1*, *pad4* and *sid2* mutants and *nahG* transgenic plants are of the Columbia (Col) ecotype. Triple mutants and transgenic plants were generated by genetic crossing. Homozygous lines were confirmed by genotyping and/or sequencing. After sterilization, seeds were sown onto Murashige and Skoog (MS) medium containing 1% sucrose and 0.8% agar, and were incubated at 4°C in darkness for 3 d, followed by irradiation for 9 h with white light to promote uniform germination. The light source in long-day and short-day conditions was cool white fluorescent lamps ($60 \mu mol\, m^{-2}\, s^{-1}$) and the temperature was maintained at 22°C.

Generation of transgenic plants
Binary vectors of *35S:HEMB1* and *pDS1301-HEMB1-amiRNA* were described previously (Tang et al. 2012). *35S:HEMB1* (to *fhy3 far1* mutant), and *pDS1301-HEMB1-amiRNA* (to No-0 wild type) were transformed via the floral dip method (Clough and Bent 1998). Transgenic plants were selected on MS plates in the presence of 50 mg/L hygromycin.

Trypan blue and DAB staining
Trypan blue and DAB staining were performed according to the method by Chen et al. (2013). After staining, tissues were mounted on slides and photographed on a dissecting microscope (Olympus).

SA determination
Leaf tissues were collected from 4-week-old soil-grown plants, weighed, and frozen in liquid nitrogen. For each sample, 0.1 g of the frozen tissue was used for measurement of free SA and SA β-glucoside (SAG). Briefly, each tissue sample was ground in liquid nitrogen, extracted with 1 mL of 90% methanol and 44 ng [^{2}H$_4$] (internal standard) and incubated at 4°C for 12 h. After centrifugation at 7600 g for 5 min, the supernatant (free SA) was dried under vacuum. The free SA sample was treated with β-glucosidase at 37°C to yield the total SA sample. For free SA and total SA determination, 0.4 mL 5% acetic/ethyl acetate and 0.4 mL H$_2$O were added, the samples were centrifuged at 7600 g for 5 min, and the supernatants were dried under vacuum. The residues were resuspended in 30 μL of methanol and 0.1 mL H$_2$O and incubated at –20°C for 2 h. The samples were then centrifuged at 13500 g for 7 min and the supernatant was dried under vacuum. The dried SA was measured using an Agilent gas chromatographer-mass spectrometer, with the separation performed in a DB-5ms column (Agilent) (Müller et al. 2002).

Bacterial growth assay
Arabidopsis plants were grown under LD (16 h light/8 h dark) conditions at 22°C for 4 weeks. Leaves were infiltrated with suspensions of *P. syringae* DC3000, *P.s.t.* DC3000 *AvrRps4*, or *P.s.t.* DC3000 *AvrRpt2* (Bent et al. 1994) at a density of 1×10^5 cfu/mL. For spray inoculation, leaves were dipped in *P.s.t.* DC3000 suspension at a density of 2×10^8 cfu/mL containing 0.05% Silwet L-77 (OSi Specialties), and were kept under high humidity. Five leaf discs (0.5 cm in diameter) were harvested 1 h (day 0) and 3 d (day 3) after inoculation and homogenized in 10 mM MgCl$_2$, and plated in serial dilutions on King's B medium containing 50 μg/mL rifampicin for selecting *P.s.t* DC3000. Plates were incubated at 28°C for 2 d, and the

colony number was then determined from three biological replicates.

Determination of ALAD activity

The activity of endogenous ALAD was determined as described previously (Tang et al. 2012).

RNA extraction and quantitative RT-PCR

Plant total RNA was extracted using an RNAprep Pure Plant Kit (Tiangen), and the first strand cDNA was synthesized by Reverse Transcriptase (Invitrogen). Real-time PCR was performed using the SYBR Premix ExTaq Kit (Takara) and a LightCycler 480 thermal cycler (Roch), following the manufacturer's instructions. Three biological replicates were performed for each sample, and the expression levels were normalized to those of *UBQ1*. All primers sequences are listed in Table S1 online.

Microarray analysis

The *fhy3 far1* mutant and No-0 wild-type plants were grown in soil under LD conditions for 4 weeks, and total RNA was isolated using the RNAprep Pure Plant Kit (Tiangen). Hybridization to the Agilent Arabidopsis Oligo Microarray (44k, Agilent Technologies) was performed according to the manufacturer's instructions. Three biological replicates were analyzed. Gene ontology (GO) terms enriched in upregulated and downregulated genes were identified with GOEAST (Zheng and Wang 2008). The *P*-value of enrichment was calculated as the hypergeometric probability of obtaining so many probes/probesets/genes for a GO term, under the null hypothesis that the probes/probesets/genes were randomly selected from the microarray/genome.

ACKNOWLEDGEMENTS

REFERENCES

Allen T, Koustenis A, Theodorou G, Somers DE, Kay SA, Whitelam GC, Devlin DF (2006) *Arabidopsis* FHY3 specifically gates phytochrome signaling to the circadian clock. **Plant Cell** 18: 2506–2516

Bartsch M, Gobbato E, Bednarek P, Debey S, Schultze JL, Bautor J, Parker JE (2006) Salicylic acid-independent ENHANCED DISEASE SUSCEPTIBILITY1 signaling in *Arabidopsis* immunity and cell death is regulated by the monooxygenase *FMO1* and the nudix hydrolase *NUDT7*. **Plant Cell** 18: 1038–1051

Bent AF, Kunkel BN, Dahlbeck D, Brown KL, Schmidt R, Giraudat J, Leung J, Staskawicz BJ (1994) RPS2 of *Arabidopsis thaliana*: A leucine-rich repeat class of plant disease resistance genes. **Science** 265: 1856–1860

Blanco F, Salinas P, Cecchini NM, Jordana X, Van Hummelen PV, Alvarez ME, Holuigue L (2009) Early genomic responses to salicylic acid in *Arabidopsis*. **Plant Mol Biol** 70: 79–102

Bray EA, Bailey-Serres J, Weretilnyk E (2000) Responses to abiotic stress. In: Buchanan BB, Gruissem W, Jones RL, eds. *Biochemistry and Molecular Biology of Plants*. American Society of Plant Physiologist, Rockville, MD. pp. 1158–1203

Caplan J, Padmanabhan M, Dinesh-Kumar SP (2008) Plant NB-LRR immune receptors: From recognition to transcriptional reprogramming. **Cell Host Microbe** 3: 126–135

Century KS, Shapiro AD, Repetti PP, Dahlbeck D, Holub E (1997) NDR1, a pathogen-induced component required for *Arabidopsis* disease resistance. **Science** 278: 1963–1965

Chen D, Xu G, Tang W, Jing Y, Ji Q, Fei Z, Lin R (2013) Antagonistic bHLH/bZIP transcription factors form transcriptional modules that integrate light and reactive oxygen species signaling in *Arabidopsis*. **Plant Cell** 25: 1657–1673

Clough SJ, Bent AF (1998) Floral dip: A simplified method for *Agrobacterium*-mediated transformation of *Arabidopsis thaliana*. **Plant J** 16: 735–743

Czarnecki O, Glaber C, Chen JG, Mayer KFX, Grimm B (2012) Evidence for a contribution of ALA synthesis to plastid-to-nucleus signaling. **Front Plant Sci** 3: 236

Eitas TK, Dangl JL (2010) NB-LRR proteins: Pairs, pieces, perception, partners, and pathways. **Curr Opin Plant Biol** 13: 472–477

Feys BJ, Moisan LJ, Newman MA, Parker JE (2001) Direct interaction between the *Arabidopsis* disease resistance signaling proteins, EDS1 and PAD4. **EMBO J** 20: 5400–5411

Fu ZQ, Dong X (2013) Systemic acquired resistance: Turning local infection into global defense. **Annu Rev Plant Biol** 64: 839–863

Gaffney T, Friedrich L, Vernooij B, Negrotto D, Nye G, Uknes S, Ward E, Kessmann H, Ryals J (1993) Requirement of salicylic acid for the induction of systemic acquired resistance. **Science** 261: 754–756

Garcia AV, Blanvillain-Baufume S, Huibers RP, Wiermer M, Li G, Gobbato E, Rietz S, Parker JE (2010) Balanced nuclear and cytoplasmic activities of EDS1 are required for a complete plant innate immune response. **PLoS Pathog** 6: e1000970

Genoud T, Buchala AJ, Chua NH, Metraux JP (2002) Phytochrome signaling modulates the SA-perceptive pathway in *Arabidopsis*. **Plant J** 31: 87–95

Hammond-Kosack KE, Jones JD (1996) Resistance gene-dependent plant defense responses. **Plant Cell** 8: 1773–1791

Heidrich K, Blanvillain-Baufume S, Parker JE (2012) Molecular and spatial constraints on NB-LRR receptor signaling. **Curr Opin Plant Biol** 15: 385–391

Hinsch M, Staskawicz B (1996) Identification of a new *Arabidopsis* disease resistance locus, RPS4, and cloning of the corresponding avirulence gene, *avrRps4*, from *Pseudomonas syringae* pv. *pisi*. **Mol Plant Microbe Interact** 9: 55–61

Hu G, Yalpani N, Briggs SP, Johal GS (1998) A porphyrin pathway impairment is responsible for the phenotype of a dominant disease lesion mimic mutant in maize. **Plant Cell** 10: 1095–1105

Hua J (2013) Modulation of plant immunity by light, circadian rhythm, and temperature. **Curr Opin Plant Biol** 16: 406–413

Hudson M, Ringli C, Boylan MT, Quail PH (1999) The FAR1 locus encodes a novel nuclear protein specific to phytochrome A signaling. **Genes Dev** 13: 2017–2027

Hudson ME, Lisch DR, Quail PH (2003) The *FHY3* and *FAR1* genes encode transposase-related proteins involved in regulation of gene expression by the phytochrome A-signaling pathway. **Plant J** 34: 453–471

Hiltbrunner A, Viczian A, Bury E, Tscheuschler A, Kircher S, Toth R, Honsberger A, Nagy F, Fankhauser C, Schafer E (2005) Nuclear accumulation of the phytochrome A photoreceptor requires FHY1. **Curr Biol** 15: 2125–2130

Ishikawa A, Okamoto H, Iwasaki Y, Asahi T (2001) A deficiency of coproporphyrinogen III oxidase causes lesion formation in *Arabidopsis*. **Plant J** 27: 89–99

Jones JDG, Dangl JL (2006) The plant immune system. **Nature** 444: 323–329

Journot-Catalino N, Somssich IE, Roby D, Kroj T (2006) The transcription factors WRKY11 and WRKY17 act as negative regulators of basal resistance in *Arabidopsis thaliana*. **Plant Cell** 18: 3289–3302

Kachroo P, Shanklin J, Shah J, Whittle EJ, Klessig DF (2001) A fatty acid desaturase modulates the activation of defense signaling pathways in plants. **Proc Natl Acad Sci USA** 98: 9448–9453

Karpinski S, Gabrys H, Mateo A, Karpinska B, Mullineaux PM (2003) Light perception in plant disease defense signaling. **Curr Opin Plant Biol** 6: 390–396

Kazan K, Manners JM (2011) The interplay between light and jasmonate signaling during defense and development. **J Exp Bot** 62: 4087–4100

Li G, Siddiqui H, Teng Y, Lin R, Wan XY, Li J, Lau NS, Ouyang X, Dai M, Wan J, Devlin PF, Deng XW, Wang H (2011) Coordinated transcriptional regulation underlying the circadian clock in *Arabidopsis*. **Nat Cell Biol** 13: 616–624

Li J, Li G, Gao S, Martinez C, He G, Zhou Z, Huang X, Lee JH, Zhang H, Shen Y, Wang H, Deng XW (2010) *Arabidopsis* transcription factor ELONGATED HYPOCOTYL5 plays a role in the feedback regulation of phytochrome A signaling. **Plant Cell** 22: 3634–3649

Lin R, Ding L, Casola C, Ripoll DR, Feschotte C, Wang H (2007) Transposase-derived transcription factors regulate light signaling in *Arabidopsis*. **Science** 318: 1302–1305

Mateo A, Muhlenbock P, Resterucci C, Chang CC, Miszalski Z, Karpinska B, Parker JE, Mullineaux PM, Karpinski S (2004) *Lesion Simulating Disease 1* is required for acclimation to conditions that promote excess excitation energy. **Plant Physiol** 136: 2818–2830

Meyers BC, Kozik A, Griego A, Kuang H, Michelmore RW (2003) Genome-wide analysis of NBS-LRR-encoding genes in *Arabidopsis*. **Plant Cell** 15: 809–834

Mochizuki N, Tanaka R, Grimm B, Masuda T, Moulin M, Smith AG, Tanaka A, Terry MJ (2010) The cell biology of tetrapyrroles: A life and death struggle. **Trends Plant Sci** 15: 488–498

Molina A, Volrath S, Guyer D, Maleck K, Ryals J, Ward E (1999) Inhibition of protoporphyrinogen oxidase expression in *Arabidopsis* causes a lesion-mimic phenotype that induces systemic acquired resistance. **Plant J** 17: 667–678

Mock HP, Heller W, Molina A, Neubohn B, Sandermann H, Grimm B (1990) Expression of uroporphyrinogen decarboxylase or coproporphyrinogen oxidase antisense RNA in tobacco induces pathogen defense responses conferring increased resistance to tobacco mosaic virus. **J Biol Chem** 274: 4231–4238

Müller A, Düchting P, Weiler E (2002) A multiplex GC-MS/MS technique for the sensitive and quantitative single-run analysis of acidic phytohormones and related compounds, and its application to *Arabidopsis thaliana*. **Planta** 216: 44–56

Nomura H, Komori T, Uemura S, Kanda Y, Shimotani K, Nakai K, Furichi T, Kohsuke Takebayashi K, Sugimoto T, Sano S, Suwastika N, Fukusaki E, Yoshioka H, Nakahira Y, Shiina T (2012) Chloroplast-mediated activation of plant immune signaling in *Arabidopsis*. **Nat Commu** 3:926

Ochsenbein C, Przybyla D, Danon A, Landgraf F, Gobel C, Imboden A, Feussner I, Apel K (2006) The role of EDS1 (enhanced disease susceptibility) during singlet oxygen-mediated stress responses of *Arabidopsis*. **Plant J** 47: 445–456

Oldroyd GE, Staskawicz BJ (1998) Genetically engineered broad-spectrum disease resistance in tomato. **Proc Natl Acad Sci USA** 95: 10300–10305

Ouyang X, Li J, Li G, Li B, Chen B, Shen H, Huang X, Mo X, Wan X, Lin R, Li S, Wang H, Deng XW (2011) Genome-wide binding site analysis of FAR-RED ELONGATED HYPOCOTYL3 reveals its novel function in *Arabidopsis* development. **Plant Cell** 23: 2514–2535

Pandey SP, Roccaro M, Schon M, Logemann E, Somssich IE (2010) Transcriptional reprogramming regulated by WRKY18 and WRKY40 facilitates powdery mildew infection of *Arabidopsis*. **Plant J** 64: 912–923

Papenbroack J, Mishra S, Mock HP, Kruse E, Schmidt EK, Petersmann A, Braun HP, Grimm B (2001) Impaired expression of the plastidic ferrochelatase by antisense RNA synthesis leads to a necrotic phenotype of transformed tobacco plants. **Plant J** 28: 41–50

Reinbothe S, Reinbothe C, Apel K, Lebedev N (1996) Evolution of chlorophyll biosynthesis — the challenge to survive photooxidation. **Cell** 86: 703–705

Shah J (2003) The salicylic acid loop in plant defense. **Curr Opin Plant Biol** 6: 365–371

Shirano Y, Kachroo P, Shah J, Klessig DF (2002) A gain-of-function mutation in an *Arabidopsis* toll interleukin 1 receptor-nucleotide binding site-leucine-rich-repeat type R gene triggers defense responses and results in enhanced disease resistance. **Plant Cell** 14: 3149–3162

Stirnberg P, Zhan S, Williamson L, Ward S, Leyser O (2012) FHY3 promotes shoot branching and stress tolerance in *Arabidopsis* in an AXR1-dependent manner. **Plant J** 71: 907–920

Stokes TL, Kunkel BN, Richards EJ (2002) Epigenetic variation in *Arabidopsis* disease resistance. **Genes Dev** 16: 171–182

Strand A, Asami T, Alonso J, Ecker JR, Chory J (2003) Chloroplast nucleus communication triggered by accumulation of Mg-protoporphyrin IX. **Nature** 421: 79–83

Strawn MA, Marr SK, Inoue K, Inada N, Zubieta C, Wildermuth MC (2007) *Arabidopsis* isochorimate synthase functional in pathogen-induced salicylate biosynthesis exhibits properties consistent with a role in diverse stress responses. **J Biol Chem** 282: 5919–5933

Tanaka R, Kobayashi K, Masuda T (2011) Tetrapyrrole metabolism in *Arabidopsis thaliana*. **The Arabidopsis Book**: e0145. doi:10.1199/tab.0145

Tanaka R, Tanaka A (2007) Tetrapyrrole biosynthesis in higher plants. **Annu Rev Plant Biol** 58: 321–346

Tang W, Ji Q, Huang Y, Jiang Z, Bao M, Wang H, Lin R (2013) FHY3 and FAR1 transcription factors integrate light and abscisic acid signaling in *Arabidopsis*. **Plant Physiol** 163: 857–866

Tang W, Wang W, Chen D, Ji Q, Jing Y, Wang H, Lin R (2012) Transposase-derived proteins FHY3/FAR1 interact with PHYTO-CHROME-INTERACTING FACTOR 1 to regulate chlorophyll biosynthesis by modulating *HEMB1* during deetiolation in *Arabidopsis*. **Plant Cell** 24: 1984–2000

Tian D, Traw MB, Chen JQ, Kreitman M, Bergelson J (2003) Fitness costs of R gene-mediated resistance in *Arabidopsis thaliana*. **Nature** 423: 74–77

Todesco M, Balasubramanian S, Hu TT, Traw MB, Horton M, Epple P, Kuhns C, Sureshkumar S, Schwartz C, Lanz C, Laitinen RAE, Huang

Y, Chory J, Lipka V, Borevitz JO, Dangl JL, Bergelson J, Nordborg M, Weigel D (2010) Natural allelic variation underlying a major fitness trade-off in *Arabidopsis thaliana*. **Nature** 465: 632–636

Vlot AC, Dempsey DA, Klessig DF (2009) Salicylic acid, a multifaceted hormone to combat disease. **Annu Rev Phytopathol** 47: 177–206

Wang H, Deng XW (2002) *Arabidopsis* FHY3 defines a key phytochrome A signaling component directly interacting with its homologous partner FAR1. **EMBO J** 21: 1339–1349

Wiermer M, Palma K, Zhang Y, Li X (2007) Should I stay or should I go? Nucleocy to plasmic trafficking in plant innate immunity. **Cell Microbiol** 9: 1880–1890

Wildermuth MC, Dewdney J, Wu G, Ausubel FM (2001) Isochorismate synthease is required to synthesize salicylic acid for plant defense. **Nature** 414: 562–565

Woodson JD, Perez-Ruiz JM, Chory J (2011) Heme synthesis by plastid ferrochelatase I regulates nuclear gene expression in plants. **Curr Biol** 21: 897–903

Wu L, Yang HQ (2010) Cryptochrome 1 is implicated in promoting R protein-mediated plant resistance to *Pseudomonas syringae* in *Arabidopsis*. **Mol Plant** 3: 539–548

Xiao Y, Savchenko T, Baidoo EEK, Chenhab WE, Hayden DM, Tolstikov V, Corwin JA, Kliebenstein DJ, Keasling JD, Dehesh K (2012) Retrograde signaling by the plastidial metabolite MEcPP regulates expression of nuclear stress-response genes. **Cell** 149: 1525–1535

Xie XZ, Xue YJ, Zhou B, Chang H, Takano M (2011) Phytochromes regulate SA and JA signaling pathways in rice and are required for developmentally controlled resistance to *Magnaporthe grisea*. **Mol Plant** 4: 688–696

Xu X, Chen C, Fan B, Chen Z (2006) Physical and functional interactions between pathogen-induced *Arabidopsis* WRKY18, WRKY40, and WRKY60 transcription factors. **Plant Cell** 18: 1310–1326

Zhang Y, Goritschnig S, Dong X, Li X (2003) A gain-of-function mutation in a plant disease resistance gene leads to constitutive activation of downstream signal transduction pathways in *suppressor of npr1-1, constitutive 1*. **Plant Cell** 15: 2636–2646

Zheng Q, Wang XJ (2008) GOEAST: A web-based software toolkit for gene ontology enrichment analysis. **Nucleic Acids Res** 36:W358–W363

Zhu Z, Xu F, Zhang Y, Cheng YT, Wiermer M, Li X, Zhang Y (2010) *Arabidopsis* resistance protein SNC1 activates immune responses through association with a transcriptional corepressor. **Proc Natl Acad Sci USA** 107: 13960–13965

SUPPORTING INFORMATION

Additional supporting information may be found in the online version of this article at the publisher's web-site.

Figure S1. Verification of *R* gene expression by qRT-PCR

Figure S2. Bacterial growth of *P.s.t.* DC3000 after spraying

Figure S3. Characterization of *HEMB1* overexpression plants in the *fhy3 far1* mutant background

Figure S4. Characterization of *HEMB1* artificial microRNA transgenic plants

Table S1. List of primers used in this study

Dataset S1. List of FHY3/FAR1-regulated genes identified in the microarray analysis Differentially regulated genes in the *fhy3 far1* mutant with a *q* value of <0.05 and a fold change of >2 are listed.